# A Robust and Secure Medical Image Watermarking Algorithm Based on Normalized DCT and Polar-coded UFMC Assisted NOMA Scheme for Telemedicine Applications

Mohammed Jabbar Mohammed Ameen[1]*      Alaa Imran Al-Muttairi[2]      Hussam Jawad Kadhim[3]

[1]*Department of Electrical Engineering, Collage of Engineering, University of Babylon, Iraq*
[2]*Department of Biomedical Engineering, Collage of Engineering, University of Babylon, Iraq*
[3]*Computer Department, College of Science for Women, University of Babylon, Iraq*
* Corresponding author's Email: drmohammedalsalihy@gmail.com

**Abstract:** This paper proposes a novel medical image watermarking scheme for a multiuser wireless system based on data normalization and polar code. The watermark image is normalized, converted into a set of coefficients using Discrete Cosine Transform (DCT), and then embedded with host medical image coefficients. The watermark image is encrypted using a Baker map and then normalized. The normalized value is converted to binary data, then XORed with a logistic map sequence, and employed as frozen bits in polar code to achieve security, robustness, and imperceptibility over the Non-Orthogonal Multiple Access-Universal Filtered Multicarrier (NOMA-UFMC) transmission scheme. A collection of medical images was employed to evaluate the proposed technique for two users, and the findings are Peak Signal to Noise Ratio (PSNR=69.5761), structural similarity index (SSIM=0.9966), mean square error (MSE=0.4399) and Normalized Cross-Correlation (NCC=0.9997) which demonstrate that it is capable of achieving a high level of imperceptibility and robustness against attacks. In addition, the proposed scheme produced good Bit Error Rate (BER) performance by exploiting the properties of polar code. Compared with the traditional techniques, the proposed approach has higher image quality, a secure watermark image, performs high robustness against various attacks, and has low execution time (about 0.3284 seconds). The suggested method is, therefore, a promising one for protecting medical images in healthcare settings.

**Keywords:** Watermarking, Medical images, DCT, Polar code, NOMA, UFMC.

## 1. Introduction

Digital existence has permeated people's lives as a result of the merge of the internet in medical devices technology. Currently, almost of medical information must be delivered over the Internet, which includes text, images, videos, and other types of media. This makes the transmitted data more vulnerable to manipulation and theft, considerably increasing the danger of patients' privacy being compromised. Thus, enhancing the security of medical data is a critical matter that must be addressed right now. The digital watermarking techniques further improve the conventional encryption techniques. It can be considered a technology for hiding information because its invisibility not only hides the patient's data but also won't influence the physician's evaluation of the host image, enhancing the safety of the patient's privacy [1]. With watermarking, specific information called a watermark is added to the host image which can later be extracted to verify its authenticity [2]. Different approaches have been devised for the secure transmission of medical images and the data that is hidden inside them. The fundamental objective is that the secret message cannot be extracted from the image by anyone but only the authorized parties. Medical image watermarking indicates the hiding of digital marks, such as the hospital's logo (name) or Electronic Patient Information (EPI). This mark aids in determining the validity of the host image and identifying ownership disputes [3]. The

watermarking approaches are categorized according to the needs of the host image in the extraction watermark image process into blind and non-blind watermarking techniques. In the blind technique, the extraction phase is independent of the host image, whereas the non-blind technique requires the host image for extraction of the watermark. Depending on the field of work, watermarking approaches can be divided into two types. One of them is the spatial domain watermarking technique, where watermark bits are inserted into the host image by altering its pixel values. The second watermarking method is the transform domain by converting the images to the frequency domain, and the embedding is done by modifying the frequency domain coefficients of the host image. In contrast to the first, the watermarking approaches using the transform domain are more powerful due to watermark is embedded by altering the coefficients within the transformation process [4]. The transforms that are most frequently used are discrete cosine transform (DCT), discrete wavelet transform (DWT), discrete Fourier transform (DFT), and singular value decomposition (SVD). The main feature of the DCT-based watermarking technique is it outperforms others due to its resistance to image compression attacks [2]. Regarding the growing demand from mobile radio users for multimedia services, higher data rates, increased bandwidth availability, and the expected increase in Internet of Things (IoT) related data traffic, the emerged of fifth-generation (5G) and Beyond 5G (B5G) wireless communication systems to address raised demands that exceed the capabilities of earlier generations of wireless networks. Non-orthogonal multiple access (NOMA) scheme has been regarded as revolutionary, capable of achieving higher spectrum efficiency and supporting a wider connection than common orthogonal multiple access approaches [5]. 5G networks rely mainly on universal filtered multicarrier (UFMC) multicarrier modulation techniques to transmit data, which minimizes peak-to-average power ratio (PAPR) and bit error rate (BER) for input data when compared with traditional wireless multicarrier modulation [6]. Polar codes are the most efficient error correction codes (ECC) techniques. Polar codes are presently employed in 5G networks and are prime candidates for B5G. The symmetry in encoding and decoding algorithms of polar code plays an important role. In addition to ECC, the modulation and multiple access schemes form the physical layer essentials [7]. To protect the transmitted data in public channels, chaotic encryption is used. Chaotic systems have distinct and desirable properties, like high sensitivity to initial conditions and control parameters [8].

This work offers the design of a watermarking algorithm to protect medical images from numerous tamperings that occur during data traffic in wireless networks by employing polar code, UFMC modulation, and DCT with the help of the NOMA scheme for multiusers over Rayleigh and Gaussian noise channels. The proposed algorithm presents simultaneously low BER, low execution time, high imperceptibility, robustness, and security levels for watermarked images that satisfy 5G requirements. This paper is structured as follows: The following section contains a list of related works. The primary focus of the proposed work is found in Section 3. Preliminaries used in the proposed scheme are given in Section 4. The significant metrics utilized in Section 5. The proposed approach is provided in Section 6, while the explanation and experimental results are provided in Section 7. In Section 8, comparisons with earlier studies are provided. In Section 9, the paper's conclusions are presented.

## 2. Related work

Many studies on image watermarking techniques have been performed. The authors in [9] present a hybrid dual watermarking (image and text) technique for healthcare setups. Dual watermarks are embedded into a radiological image utilizing a DWT-SVD based on a watermarking approach. Hamming, BCH, Reed–Solomon (RS), and hybrid ECC are applied to improve the robustness of the watermark medical image. The experimental findings of the suggested method are Peak Signal to Noise Ratio (PSNR) = 37.87 and Normalized Cross-Correlation (NCC) 0.8994 at gain factor =0.05 for hybrid model and tested under different attack types. The limitations of this algorithm are the encryption process and execution time, which are not being considered.

In [10], the authors presented a selective DWT supported by a spread-spectrum watermarking algorithm for embedding medical image. The DWT coefficient is selected for the embedding phase using a threshold of the coefficient values in the column. The host and watermark images have been embedded in selection coefficients for the first- and second-level DWTs, respectively. BCH was applied before embedding to enhance the robustness. The findings are PSNR =37.75 and NCC= 0.6148 at a gain factor of 0.5, and they were also tested under various attack types. The limitations of this method are low PSNR and NCC, and the execution time is not considered.

The authors in [11] suggested a blind medical image watermarking algorithm based on Fast Discrete Curvelet Transform (FDCuT) and DCT. FDCuT is employed on a medical image to obtain

various frequency coefficients of its curvelet decomposition. The high frequency coefficients of FDCuT are applied to DCT, while mid-band frequency coefficients are modified by Gaussian Noise. The simulation results are PSNR = 55.06 and NCC = 0.9230 at a gain factor of 2, execution time = 29.95, and were tested under various geometric attacks. The fact that this method employs no security measures is one of its limitations, as well as the high processing time.

The authors in [12] produced an approach for multiple watermarking based on DWT, DCT and SVD for healthcare setups. For identification issues, the suggested approach utilizes three medical watermarks in the form of a Lump image, the doctor's signature and the diagnostic information of the patient. The robustness is improved by using a back propagation neural network on the extracted image to minimize the effects of noise. Also, the security is increased by applying Arnold transform prior to embedding process into the host image. Further, doctor signature and diagnostic information watermark images are also encoded by Hamming code and arithmetic encoding technique, respectively. The simulation results illustrate that the suggested approach has PSNR= 43.88 and NCC= 0.9547 at a gain factor of 0.01, and it is also tested under different attacks. The limitation of this method is that execution time is not considered.

In [13], the authors presented a combined DCT and successive division based on host and watermark image schemes, respectively. The findings are PSNR = 51.6464 and NCC= 0.9997, and they were also tested under cropping attack only; the proposed method has good imperceptibility and a low execution time of 0.463. This technique's drawback is that it doesn't employ any security features.

The researchers in [14] present an image watermarking algorithm by applying block-based DCT coefficient alteration. The difference between the DCT coefficients of the two blocks is determined and modified depending on the watermark bit to bring it within a preset range. The suggested method has a PSNR of 41.66 and was tested under different attacks, but the execution time is not considered.

The authors in [15] introduced a medical image watermarking method by combining DWT and SVD to protect the image exchange via telemedicine and avoid any confusion between patient data. The experimental results of the suggested scheme are PSNR = 57.04, SSIM = 0.9998, and MSE = 0.1251. In addition, it has been tested under different attacks and has good robustness, but the execution time and BER are not considered.

The researchers in [16] present an image watermarking scheme that utilizes DWT-SVD in the Fractional Order Fourier Transform (FRFT). The experimental evaluation of PSNR = 57.31 and SSIM = 0.87 under no attacks, whereas the limitation of this method did not consider the execution time and encryption process.

In [17], the authors suggested an image watermarking scheme by embedding a stego-text into the least significant bit (LSB) of the DCT coefficient by utilizing a linear modulation algorithm. The findings are PSNR = 43.30, NCC = 1, and SSIM = 0.9937 under no attacks, whereas the limitation of this scheme did not consider the execution time and use of security features.

The previously stated approaches lack crucial features required to make a balanced tradeoff in the performance of the watermarking algorithm, including imperceptibility, robustness, security, BER, and processing time for the embedding and extraction processes. In order to fulfill all the mentioned requirements, a secure image watermarking technology is proposed that provides high imperceptibility and robustness against attacks. Also, very low processing time, compatibility with high-speed networks, low BER, and better privacy for patients' identities.

## 3. Research contributions

The contributions of this research are as follows:
I. High imperceptibility, robustness, and security were obtained for the proposed watermarking algorithm compatible with 5G networks used in telemedicine and telediagnosis applications.
II. The polar code achieves additional robustness for sensitive data and improves BER performance.
III. A novel, efficient, simple image watermarking based on DCT for multiusers is developed using data normalization to overcome high computation costs, processing time problems, and signal recovery quality.
IV. The proposed approach is robust against geometric attacks.

## 4. Preliminary

### 4.1 NOMA scheme

NOMA has evolved a significant approach for 5G wireless networks due to massive connectivity and high data rate. NOMA scheme can be performed power-domain (PD), code-domain (CD) or multiple domains. The superposition coding (SC) principle is used in PD-NOMA to transmit data of numerous
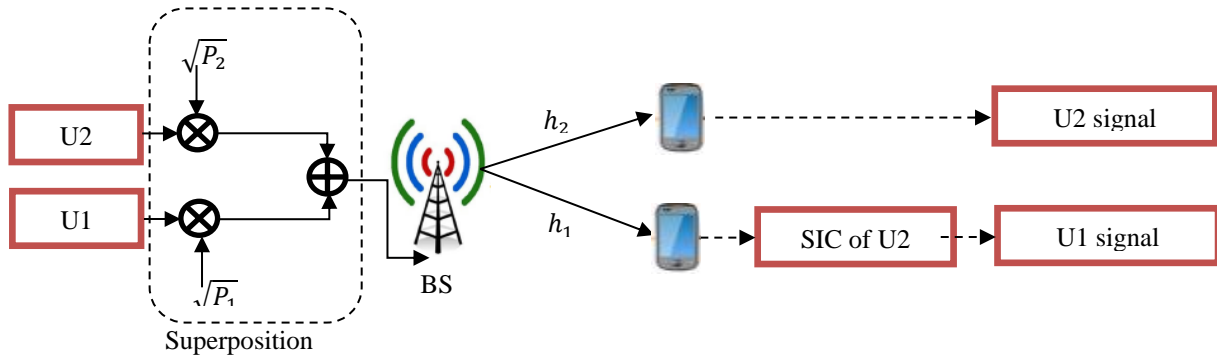
68



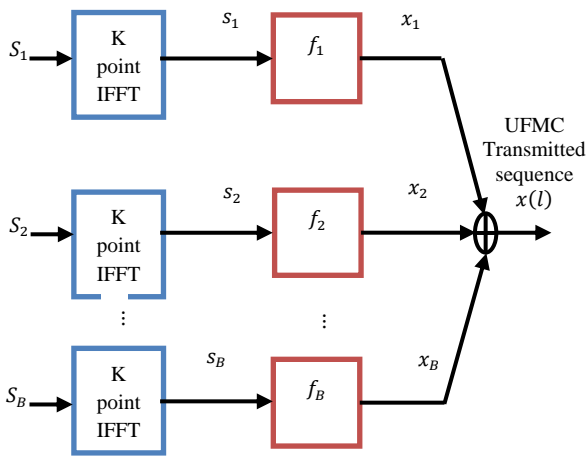Figure. 1 Two-user downlink system of the NOMA scheme [18]



Figure. 2 Block diagram of the general UFMC scheme [20]

users using a single time-frequency resource. The downlink multiuser is identified by assigning different power at the transmitter, and a successive interference cancellation (SIC) method is used at the receiver side for decoding data from distinct users. As shown in Fig. 1, the downlink PD-NOMA case in the base station (BS) with two users is regarded, where $U_1$ and $U_2$ are near user and far user, respectively. SC is done at the BS to transmit data with different power is represented as:

$$s = \sqrt{P_1}s_1 + \sqrt{P_2}s_2$$
$$= \sqrt{\alpha P}s_1 + \sqrt{(1-\alpha)P}s_2 \qquad (1)$$

By assuming that the total power, denoted as P, is normalized to unit energy for analysis simplicity. The power allocation factor (PAF) is represented by $\alpha$ with $P_1 = \alpha$ P and $P_2 = (1-\alpha)$ P. The symbols $s_1$ and $s_2$ represent the transmitted signals from the BS to $U_1$ and $U_2$, respectively. The received signal at $U_\theta$ can be described as follows:

$$r_\theta = h_\theta . s + v_\theta, \ \theta = 1,2 \qquad (2)$$

where $h_\theta$ and $v_\theta$ represents the channel response, when $|h_1|^2 > |h_2|^2$, indicating that the channel condition for the near user ($U_1$) is stronger than that for the far user ($U_2$). As a result, the stronger user gets less transmit power, while the weaker user gets more. On the user end, the signal $U_2$ is initially decoded by treating the signal $U_1$ as interference because it has a larger share of transmit power. The signal $U_1$ can then be decoded by conducting SIC to remove $U_2$ from received signal, as follows:

$$r_1 = h_1 . s + v_1 - h_1\sqrt{P_2}\hat{s}_2$$
$$= h_1 . \left(\sqrt{P_1}s_1 + \sqrt{P_2}s_2\right) + v_1 - h_1\sqrt{P_2}\hat{s}_2 \qquad (3)$$

where $\hat{s}_2$ indicates a demodulated signal of $U_2$ [18].

### 4.2 UFMC transmission scheme

UFMC is one of the candidate technologies to satisfy 5G networks. The waveform of UFMC distributes several subcarriers into sub-bands. As a result, the cyclic prefix and out-of-band emission are reduced, which improves the spectral efficiency. UFMC is a scheme that filters blocks of subcarriers before their being transmitted and received to eliminate inter-carrier and inter-symbol interferences. UFMC stands as a modulation technique encompassing attributes of both a generalized filter bank multicarrier technique (FBMC) and filtered OFDM. Within the UFMC system, there exists a straightforward adaptability to customize the subband width and filter length, thereby aligning with the precise demands of individual users [19].

As shown in Fig. 2, a multicarrier system with $N$ total number of subcarriers is partitioned into $B$ subbands, with each subband including many successive subcarriers, i.e., each subband contains $K = N/B$ subcarriers. In theoretical terms, the number of carriers in the $i^{th}$ subband is $K_i$, for $i = 1, 2,.., B$. In fact, for purposes of simplicity, normally divides each sub-band equally. Foremost, specific

69
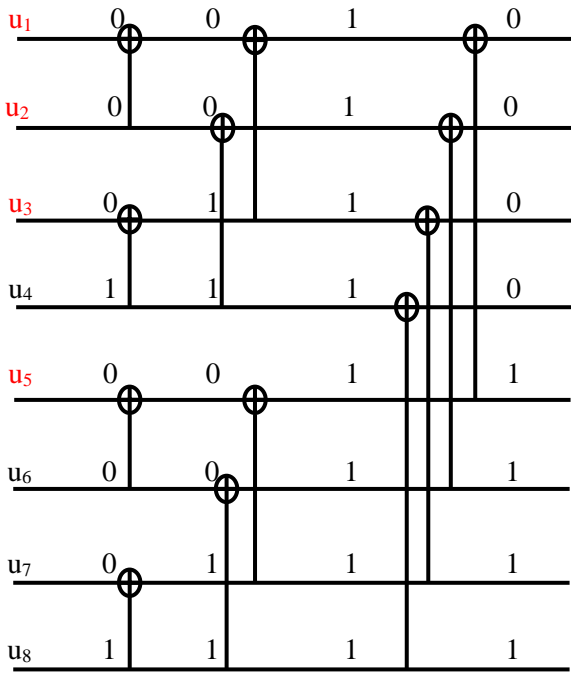


Figure. 3 Polar code encoding: $N = 8$, $k = 4$, $F = [1,2,3,5]$, $uF = (0,0,0,0)$ and $uFc = (1,0,0,1)$. The result codeword is $x = (0,0,0,0,1,1,1,1)$ [21]

information bits are mapped to symbols using M-QAM. These symbols are allocated to each subband using average carrier allocation. For the $i^{th}$ subband, the symbols allocated in the frequency range are $Si$ and their length is $K_i$. Then, these symbols are converted into time domain signals $S_i$ via N-point inverse fast Fourier transform (IFFT). Notice how IFFT differs from traditional transformations here. According to the IFFT module, the time domain signal $S_i$ of the $i^{th}$ subband can be represented as:

$$s_i(l) = \frac{1}{\sqrt{N}}\sum_k S_i(k)e^{\frac{i2\pi kl}{N}}$$
$$l = 0,1,\dots,N-1 \tag{4}$$

After that, each subband is filtered. The discrete time signal is created by adding signals from filtered subbands. As a result, the superposition of all subband symbols, i.e. the transmitted signal $x$, may be described as:

$$x(l) = \sum_{i=1}^{B} s_i(l) * f_i(l)$$
$$l = 0,1,\dots,L+N-2 \tag{5}$$

Where $*$ indicates convolution operation, $S_i(l)$ is a signal in time domain, $f_i(l)$ is impulse response of the FIR filter and L represents the length of the filter [20].

## 4.3 Polar code

Arikan first introduced the polar code in 2009. It is generally a new type of error-correcting linear block code. Polar codes are based on the phenomena of channel polarisation, which is an important factor in reaching Shannon's capacity. Channel polarisation is strategy of spreading channel capabilities across distinct instances, or more accurately uses, of a communication channel while preserving entire capacity.

Polar codes generate a range of good and bad channels, allowing data bits to be sent across the good channels whereas the entry to the bad channels is frozen. Let the input vector $u = [u_1, u_2, \dots, u_N]$, a polar code encodes k data bits into N coded bits using (N - k) redundant bits, which are often known as 'frozen bits. Polar code is usually defined by the parameters *(N, k,F, uF)*, where $F \in \{1, 2, \dots N\}$ indicates the position of frozen bits, while *uF* is *(N - k)* bits of frozen bits, which are well-known at the decoder , therefore, these parameters determine its performance.. For any encoder $G_N$, the polar encoding process can be characterised as follows:

$$x = uG_N \tag{6}$$

Where $G_N$ is the $n^{th}$ Kronecker product of the $(2 \times 2)$ kernel matrix, which represents the encoding transformation $G_2$. More precisely, Arikan's kernel $G_2$ may be described in matrix notation as:

$$G_2 = \begin{bmatrix} 1 & 0 \\ 1 & 1 \end{bmatrix} \tag{7}$$

while the *N*-bit encoder $G_N$ is described as:

$$G_N = G_2^{\otimes n} = \begin{bmatrix} G_{N/2} & 0 \\ G_{N/2} & G_{N/2} \end{bmatrix} \tag{8}$$

As a result, Arikan's polar code has a recursive configuration that invokes $n = log_2 N$ layers of polarization, with each layer employing *N/2* XOR gates. For instance, consider the following 8-bit polar code: $k = 4$, $F = [1, 2, 3, 5]$, $uF = (0,0,0,0)$, and a data bit sequence $u_{Fc} = (1,0,0,1)$. The encoded output can then be calculated using the formula below:

$$\left. \begin{aligned} x &= (0\ 0\ 0\ u_4\ 0\ u_6\ u_7\ u_8).G_8 \\ x &= (0\ 0\ 0\ 1\ 0\ 0\ 0\ 1).G_8 \\ x &= (0\ 0\ 0\ 0\ 1\ 1\ 1\ 1) \end{aligned} \right\} \tag{9}$$

*Fc* indicates the complementary set of *F*, which determines the position of data bits. The codeword of

70

Eq. (9) can also be obtained straight from the encoding circuit, as shown in Fig. 3. The encoding mechanism of Eq. (6) may be rephrased as:

$$x = u_{FC}G_N(FC) + u_F G_N(F) \qquad (10)$$

where $G_N(F)$ is a sub-matrix of $G_N$ having only the rows with indices in $F$. The polar decoder is based on successive cancellation algorithms [21].

## 4.4 Discrete cosine transform (DCT)

DCT is an interesting transformation technique that converts data from spatial (time) to frequency domain. DCT was substantially used for image processing challenges due to its energy compaction feature. The majority of the energy is centred at lower frequencies, then the coefficients of higher frequencies can be eliminated without causing too much data quality degradation. The DCT and its inverse can be expressed in the following mathematical formula:

$$
C(u,v) = \frac{2}{\sqrt{mn}}\alpha(u)\alpha(v)\sum_{x=0}^{m-1}\sum_{y=0}^{n-1}f(x,y)
$$
$$
\times cos\frac{(2x+1)u\pi}{2m} \times cos\frac{(2y+1)v\pi}{2n} \qquad (11)
$$

$$
f_i(x,y) = \frac{2}{\sqrt{mn}}\sum_{u=0}^{m-1}\sum_{v=0}^{n-1}\alpha(u)\alpha(v)f(x,y)
$$
$$
\times cos\frac{(2x+1)u\pi}{2m} \times cos\frac{(2y+1)v\pi}{2n} \qquad (12)
$$

where $f(x,y)$ indicates the pixel value in the time domain, $C(u,v)$ is the DCT coefficient, m and n denote the block size , and

$$
\alpha(u), \alpha(v) = \begin{cases} 1/\sqrt{2} \ if \ u,v = 0 \\ 1 \qquad\qquad else \end{cases} \qquad (13)
$$

When substituting $u = v = 0$ into Eq. (11) will be obtained the DC coefficient value and all other coefficients are referred to as the AC coefficients [22].

## 4.5 Watermark encryption

The security of the watermark image is critical if the watermark is to survive against unauthorized access. In general, robust watermarking is insufficient to protect sensitive information from various attacks, when the embedding algorithm is broken down in any way by an unauthorized person, the information is destroyed. The encryption approach guarantees that no one can access to confidential information without providing the key employed in the encryption procedure. Chaos encryption proves to be the most suitable encryption method to protect secret data and ensure data security. Chaos mapping has characteristics such as irreversibility, pseudo-randomness, and dynamic behaviour. One of the most often utilized chaotic maps in image encryption is the Baker map. A 2-D Baker map equation is as follows:

$$
(x_{n+1}, y_{n+1}) =
\begin{cases}
\left(\frac{x_n}{p}, , py_n\right) & , 0 < x \le p \\
\left(\frac{(x_n-p)}{(1-p)}, (1-p)y_n + 1 - p\right) & , p < x \le 1
\end{cases} \qquad (14)
$$

where $p$ is the system parameter; $x_n$ and $y_n$ indicate the state variables. A Baker map can produce two chaotic sequences [23]. Also, another simple and efficient chaotic map is named the logistic map and can be represented by the following equation:

$$X_{n+1} = rX_n(1 - X_n) \qquad (15)$$

The parameter r takes a value in the range $3.57 \le r \le 4$ and $x_n$ represents the state variables [24].

## 4.6 Image normalisation

There are numerous pre-processing techniques available to normalize medical images before image analysis. The process of changing the range of pixel intensity values in an image is known as image normalization. The simplest form of normalization is linear normalization, which simply divides each pixel value by the maximum value that a pixel may take. If an image is 8-bit, for instance, each pixel value will be in the range [0, 255]. Linear normalization would divide each pixel value by 255, resulting in a pixel value range of [0, 1]. Some of the advantages of image normalization include: reducing image noise and increasing image processing [25].

## 5. Imperceptibility and robustness analysis

Imperceptibility is an important metric that indicates the variations of the quality between a host image prior to and after the embedding process. The values of components such as NCC, SSIM, and PSNR are commonly used to calculate imperceptibility.
NCC test is used to examine the relationship between the host image and the extracted watermark. Let a watermark ($W_I$) of size N × N, then NCC can be calculated as:
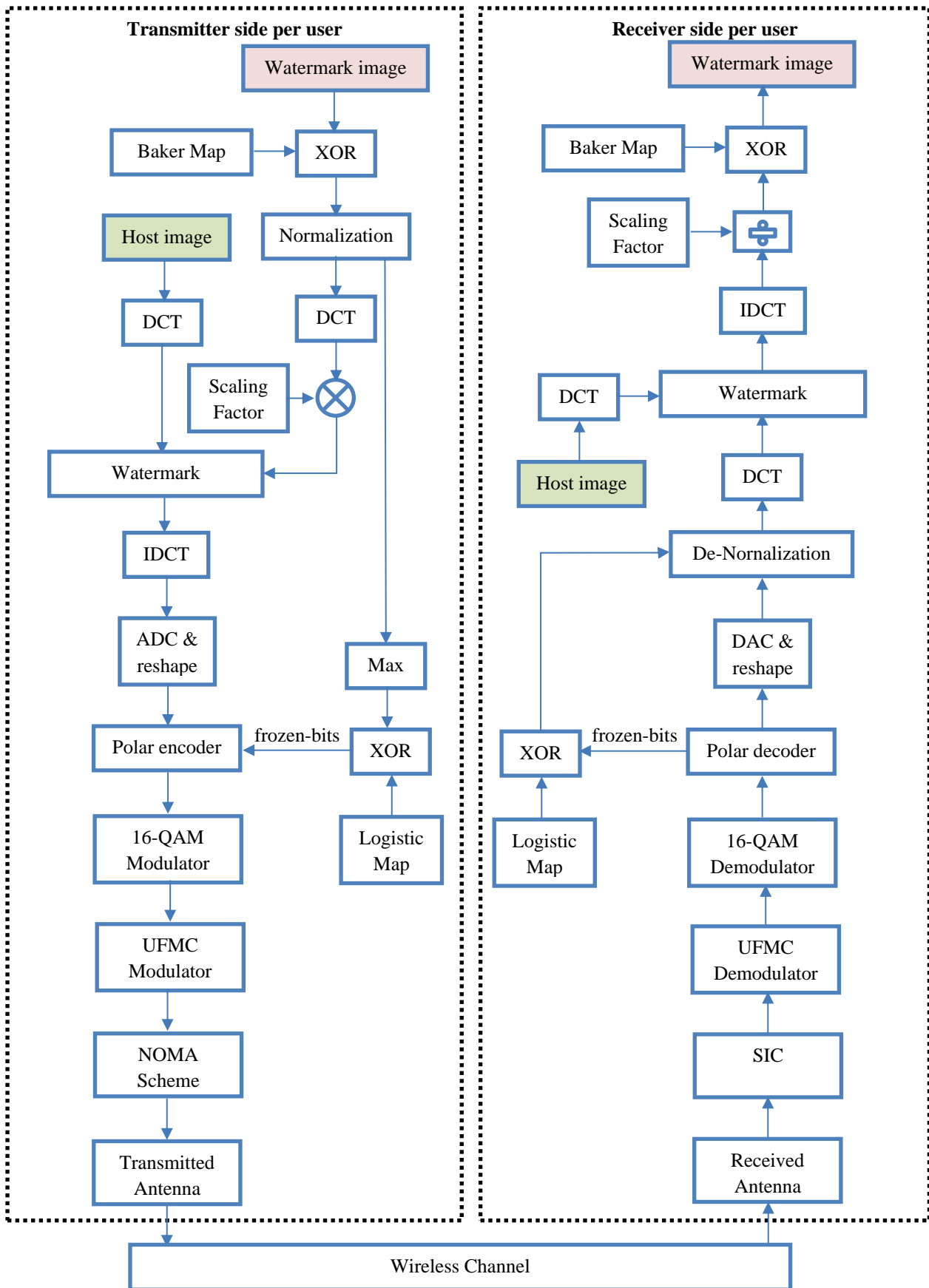
Figure. 4 Block diagram of image watermarking with embedding and extraction processes of the proposed Normalized DCT and Polar-coded UFMC Assisted NOMA scheme per user

$$NCC = \frac{\sum_{i=1}^{N}\sum_{j=1}^{N} W_1(i,i) \times W_1^*(i,j)}{\sum_{i=1}^{N}\sum_{j=1}^{N}[W_1(i,i)]^2} \qquad (16)$$

Where $W_1$ and $W_1^*$ are original and extracted watermark images, respectively. The SSIM index is used to determine the degree of similarity between the host image ($W_2$) and its watermarked version ($W_3$), SSIM can be described as:

$$SSIM = l(W_3, W_2) c(W_3, W_2) \, s(W_3, W_2) \qquad (17)$$

Where $l(W_3, W_2)$, $c(W_3, W_2)$, $and \, s(W_3, W_2)$ are comparison functions of luminance, contrast, and structure, respectively. While, for an image with dimensions of M × M, M=512, the PSNR is defined as:

$$PSNR = 10 \, log_{10} \frac{M \times M \times max[W_2(i,j)]^2}{\sum_{i=1}^{M}\sum_{j=1}^{M}[W_2(i,i) - W_3(i,i)]^2} \qquad (18)$$

In addition, the mean square error (MSE) between the host image and the watermarked image $W_3$ is expressed as:

$$MSE = \sum_{i=1}^{M}\sum_{j=1}^{M}[W_2(i,i) - W_3(i,i)]^2 \qquad (19)$$

Both SSIM and NCC have values ranging from 0 to 1. Furthermore, a higher SSIM value indicates better watermark invisibility, while a higher NCC value indicates stronger robustness. A high PSNR value is preferred since it implies that there is a tiny difference between the host and the watermarked image. Several geometric attacks try to erase or hide a watermark image from a host image in order to test the scheme's robustness [26]. The main attack types used in this work are average filter, rotation, crop, histogram equalization, gaussian noise, and median filter.

## 6. Proposed watermarking algorithm

This part provides a detailed description of the suggested watermarking technique for secure medical image exchange. The block diagram of the proposed watermarking technique is shown in Fig. 4, which includes normalized DCT and Polar-coded UFMC Assisted NOMA scheme, which are implemented to create a new imperceptible, robust and simple watermarking technique to fulfill copyright protection. The proposed approach works well and satisfies the requirements for imperceptibility, security, and robustness of different attacks; therefore, it is appropriate for medical images exchanged in telemedicine applications.

### 6.1 Watermark embedding algorithm

The watermark image ($W_1$) used in this scheme is a 64 × 64 embedded in a 512 × 512 host image ($W_2$). The steps of the proposed embedding process are as follows:

**Step 1**: The host and watermark images should be converted to grayscale images.
**Step 2**: Apply 16-bit analogue to digital converter (ADC) to the watermark image.
**Step 3**: Reshape the sequence of the Baker map to a 64 × 64 matrix and apply 16-bit ADC.
**Step 4**: Perform XOR operation between **Step 2** and **Step 3**
**Step 5**: Convert bits in **Step 4** to decimals using a 16-bit digital-to-analogue converter (DAC).
**Step 6**: Apply the DCT host image.
**Step 7**: Normalize the watermark image and apply the DCT.
**Step 8**: Divide the host image into 8×8 square blocks.
**Step 9**: $W_1$ is inserted into $W_2$ as follows:
Watermarked image ($W_3$) =$W_1$+a×$W_2$, a: Watermark embedding intensity
**Step 10**: Apply IDCT to the watermarked image.
**Step 11**: Convert the normalized value of the watermark image to binary using 16-bit ADC.
**Step 12**: Convert the chaotic sequence of the Logistic map to 16 bits/ sample.
**Step 13**: Apply XOR between **Step 11** and **Step 12**.
**Step 14**: Use frozen bits of the polar encoder from **Step 13** after padding.
**Step 15**: Apply 16-QAM modulator.
**Step 16**: Reshape data into 16 subbands and each of 16 subcarriers to perform the UFMC modulation scheme.
**Step 17**: Apply PAF for each user to achieve the NOMA scheme; for user 1, PAF=0.25, and user 2, PAF=0.75.

### 6.2 Watermark Extraction Algorithm

The received watermarked image ($W_3$) of size 512 × 512 can be extracted in the following steps:
**Step 1**: Appling SIC to decode data for the specified user.
**Step 2**: Reshape data into 16 subbands and each of 16 subcarriers to perform the UFMC demodulation scheme.
**Step 3**: Apply 16-QAM demodulator.
**Step 4**: Apply successive cancellation decoder, location of frozen bits, known to the decoder.
**Step 5**: Select frozen bits of the polar decoder from **Step 4** after removing zero padding.
**Step 6**: Convert the chaotic sequence of the Logistic map to 16 bits/ sample.

73

**Step 7**: Perform XOR between **Step 5** and **Step 6**.
**Step 8**: Convert bits in Step 7 to decimals using a 16-bit DAC.
**Step 9**: Convert bits in **Step 4** to a decimal using 16-bit DAC.
**Step 10**: Multiplying Step 9 by Step 8.
**Step 11**: Apply DCT.
**Step 12**: Extract the watermark as follows:

$$W_2 = \frac{W_3 - W_1}{a}$$

**Step 13**: Apply IDCT.
**Step 14**: Apply 16-bit ADC to the extracted watermark.
**Step 15**: Apply 16-bit ADC to the Baker map.
**Step 16**: Perform XOR between **Step 1** and **Step 15**.
**Step 17**: Apply 16-bit DAC to **Step 16**.

## 7.  Simulation results

This section analyses the proposed watermarking technique evaluation by measuring watermark imperceptibility and robustness. MedPix® was used to take a variety of medical images for analysis. With Matlab R2020 software running in Windows 10 and an Intel(R) Core (TM) i7-7500U laptop with 2.70 GHz 2.9 GHz, 8 GB RAM, and a 64-bit operating system, the suggested scheme was implemented. The proposed watermarking technique was tested under numerous medical images with and without various attacks. Table 1 parameter values used through simulation.

Table 1. parameters for simulations

| Scheme | Parameter | Value |
|---|---|---|
| UFMC | Total Number of subcarriers(N) | 256 |
| | Number of sub-band (B) | 16 |
| | Number of subcarriers per sub-band (K) | 16 |
| | Filter type | Dolph Chebyshev |
| | Side Lobe Attenuation | 40 dB |
| | Modulation scheme | 16-QAM |
| | Number of bits per subcarrier | 4 |
| NOMA | Number of users | 2 |
| | Power allocation factor (PAF) | 0.25 |
| | Channel Fading | Rayleigh-Flat |
| Polar code | Length of polar code (N) | 32 bits |
| | Number of information (k) | 12 bits |
| | Number of frozen (N-k) | 20 bits |
| ADC | Bits/sample | 16 |

### 7.1 Imperceptibility test

NCC, SSIM, PSNR, and MSE metrics have been used to evaluate the imperceptibility of the watermarked image yielded by the suggested scheme. Fig. 5 shows the host, watermark, and watermarked images with their corresponding watermarks extracted from them. Table 2 presents the objective metrics of watermarked images acquired by the suggested technique for two users.

It is evident from the findings above that the watermarked image's average PSNR value is higher than 68 dB, and NCC with approximately unity value has been obtained. In addition, the extracted image cannot be decrypted if the receiver knows the embedding algorithm unless it has a decryption secret key. Therefore, it is clear that high imperceptibility is preserved for watermarked images, and thus, the scheme can be applied in many medical image exchanges.

### 7.2 Robustness test

Watermarked images are subjected to different attacks to evaluate the proposed algorithm's resilience.

The robustness of the approach is thought to be high for that attack if the retrieved watermark is reasonably identifiable. The outcomes of multiple attacks on the watermarked image in terms of PSNR and NCC are shown in Fig. 6. The findings shown in Fig. 6 make it evident that the suggested scheme has strong resilience and can effectively defend against all of the attacks indicated.

### 7.3 Processing time analysis

The processing time of this scheme depends on the size of the host image and the watermark used.

The larger the image dimensions, the longer the processing time. In addition, the total processing time of the watermark processing is measured as the sum of the respective times required for the embedding and extraction processing. The processing time evaluation of the proposed method is shown in Table 3.

### 7.4 Performance analysis

The proposed scheme uses polar code within the embedding algorithm and as ECC to enhance the system performance in terms of BER. The BER metric measures the amount of incorrect bits that were retrieved from the received image through the wireless channel. A lower BER indicates the effectiveness of the transmission system and
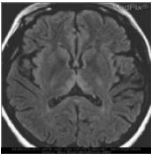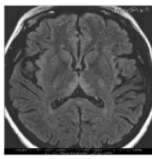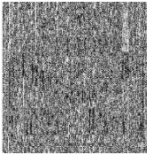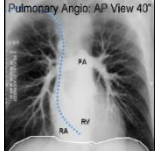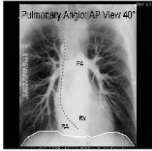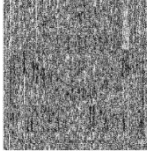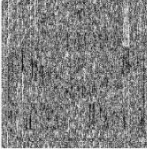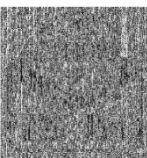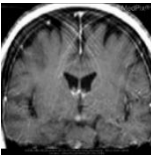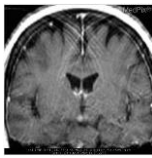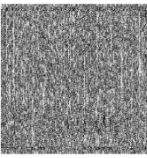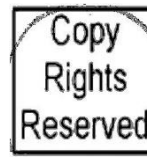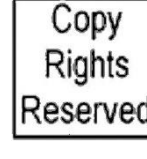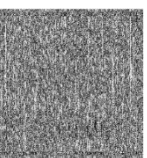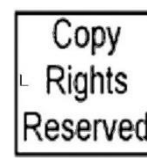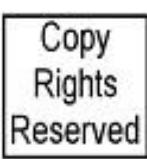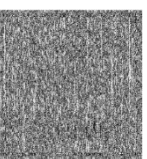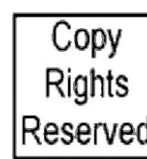
| | Name | Host Image | Watermark Image | Watermarked Image | Extracted Encrypted watermark | Extracted Decrypted watermark |
|---|---|---|---|---|---|---|
| User 1 | Brain | | | | | |
| | Chest | | | | | |
| | Hand | | | | | |
| | Knee | | | | | |
| User 2 | Brain | | | | | |
| | Chest | | | | | |
| | Hand | | | | | |
| | Knee | | | | | |

Figure. 5 watermarked and extracted images without attacks
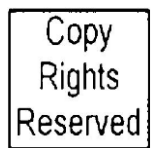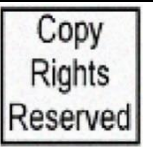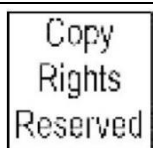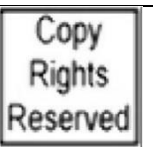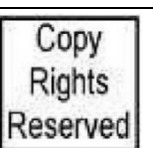
| Attacks type | User 1 | | User 2 | |
| --- | --- | --- | --- | --- |
| | Watermarked image | Extracted watermark | Watermarked image | Extracted watermark |
| average filtering using 3× 3 pixels neighborhood |  |  |  |  |
| | PSNR= 50.0199 | NCC= 0.9835 | PSNR= 48.9777 | NCC= 0.9896 |
| rotation with 30◦ anticlockwise |  |  |  |  |
| | PSNR=33.9435 | NCC= 0.9832 | PSNR=33.2363 | NCC= 0.9855 |
| Gaussian noise with zero mean and 0.01 variance |  |  |  |  |
| | PSNR= 29.273 | NCC= 0.9471 | PSNR= 28.8201 | NCC= 0.9428 |
| Cropping one-fourth from the left side |  |  |  |  |
| | PSNR= 20.5427 | NCC= 0.9775 | PSNR= 20.2471 | NCC= 0.9698 |
| histogram equalization |  |  |  |  |
| | PSNR=11.3219 | NCC= 0.9537 | PSNR= 11.2239 | NCC= 0.9529 |
| median filtering using 3 × 3 pixels neighborhood |  |  |  |  |
| | PSNR= 36.2816 | NCC=0.9745 | PSNR= 36.1742 | NCC=0.9749 |
| JPEG compression with a quality factor of 50 |  |  |  |  |
| | PSNR= 48.3865 | NCC=0.9754 | PSNR=48.2637 | NCC=0.9767 |

Figure. 6 Watermarked and extracted watermark imaged against various attacks

Table 2. Perceptual quality metrics of watermarked medical images under no attacks

| image | User 1 | | | | User 2 | | | |
|---|---|---|---|---|---|---|---|---|
| | NCC | SSIM | PSNR | MSE | NCC | SSIM | PSNR | MSE |
| Brain | 0.9997 | 0.9966 | 69.5761 | 0.4399 | 0.9908 | 0.9890 | 68.1254 | 0.3363 |
| Chest | 0.9934 | 0.9361 | 69.5371 | 0.3864 | 0.9966 | 0.9824 | 68.0008 | 0.2905 |
| Hand | 0.9924 | 0.9242 | 69.5425 | 0.3846 | 0.9948 | 0.9831 | 68.0119 | 0.3856 |
| Knee | 0.9998 | 0.8876 | 69.5884 | 0.3930 | 0.9970 | 0.8946 | 67.9884 | 0.3959 |

Table 3. Processing time evaluation

| Image /user | Image size | Embedding Time | Extraction Time | Total Time |
|---|---|---|---|---|
| Knee /user 1 | 28.6 KB | 0.206 (Sec.) | 0.1224 (Sec.) | 0.3284 (Sec.) |
| Knee /user 2 | 30.2 KB | 0.215 (Sec.) | 0.1295 (Sec.) | 0.3445 (Sec.) |



Figure. 7 BER performance of the proposed polar coded UFMC assisted NOMA system

embedding algorithm. As shown in Fig. 7, two scenarios are investigated, the first one is a watermarking algorithm using traditional DCT with UFMC-assisted NOMA scheme for two users, whereas the second one is a watermarking algorithm using normalized DCT with polar coded UFMC-assisted NOMA scheme for two users. It is clear that the proposed scheme gives a very low BER and thus reduces the channel distortion.

## 8.  Comparative study

This section illustrates a comparison between the proposed algorithm and other popular algorithms found in the literature. Table 4 presents the database and parameters used in the past studies, while Table 5 lists the PSNR and NCC values of the extracted watermarks with and without attacks. The host image used in Table 5 is the Knee image of user 1. As observed in the table, the watermarked images produced by the suggested approach have greater PSNR values than the other works. It means that the host image suffers less distortion as a result of the watermark insertion. The images that are received may be damaged by different attacks after being transmitted over a wireless channel for each user. Thus, under attacks, the comparison will be performed in terms of NCC. The watermarked image of the proposed algorithm that is subjected to Average Filtering, Rotation, Cropping, and JPEG Compression attacks is more robust than other schemes, whereas it gives acceptable robustness when subjected to Gaussian Noise, Histogram Equalization, and Median Filtering attacks. In addition, the average total execution time for the proposed algorithm is about 0.3284 Sec. When

Table 4. Database and parameters of previous works

| Reference \ Parameter | [9] | [10] | [11] | [12] | Proposed |
|---|---|---|---|---|---|
| Host image size | 512×512 | 512×512 | 1024 × 1024 | 512×512 | 512×512 |
| Watermark image size | 256×256 | 64×20, 80×25, 99×31 | 128 × 128 | 256×256 | 64×64 |
| Transform for Watermark Embedding | DWT+SVD | DWT | FDCuT+DCT | DWT+DCT+SVD | Normalized DCT |
| Gain factor | 0.01 to 0.1 | 1 to 5 | 2 to 8 | 0.01 to 0.2 | 0.01 |
| Colorimetry | grayscale | grayscale | grayscale | grayscale | grayscale |
| Security mechanism | - | Spread Spectrum | Gaussian Noise | Arnold transform | Baker Map |
| ECC | BCH+RS+ Hamming code | BCH | - | Hamming code | Polar code |

Table 5. Robustness and processing time comparison with previous works for user 1 and Knee image

| Reference | [9] | | [10] | | [11] | | [12] | | Proposed | |
|---|---|---|---|---|---|---|---|---|---|---|
| Metrics | PSNR | NCC | PSNR | NCC | PSNR | NCC | PSNR | NCC | PSNR | NCC |
| No Attack | 37.87 | 0.8994 | 37.75 | 0.6148 | 55.06 | 0.9230 | 43.88 | 0.9547 | 69.5884 | 0.9998 |
| Average Filtering | - | - | - | - | - | 0.8688 | - | - | 50.0199 | 0.9835 |
| Rotation | - | - | - | - | - | 0.7895 | - | - | 33.9435 | 0.9832 |
| Gaussian Noise | - | 0.3289 | - | 0.7394 | - | 0.9322 | - | 0.9466 | 29.273 | 0.9471 |
| Cropping | - | 0.9481 | - | - | - | 0.9704 | - | - | 20.5427 | 0.9775 |
| Histogram Equalization | - | 0.8187 | - | 0.7402 | - | 0.9689 | - | 0.9404 | 11.3219 | 0.9537 |
| Median Filtering | - | - | - | 0.2162 | - | 0.9538 | - | - | 36.2816 | 0.9745 |
| JPEG Compression | - | - | - | 0.7364 | - | 0.7125 | - | 0.9787 | 48.3865 | 0.9754 |
| Total execution time (Sec.) | - | | - | | 29.95 | | - | | 0.3284 | |

compared with other competing algorithms, it is also efficient in terms of computational time and compatible with modern high-speed communication networks.

## 9. Conclusions

A new approach to the watermarking technique, which uses normalized DCT and is compatible with modern communications networks for multiusers, is proposed in this work. The watermark image is encrypted employing a Baker map before embedding and then normalized, the normalized value of an encrypted image is mixed with a chaotic Logistic map, and then, the secure sequence is employed in polar code as frozen bits. The embedded medical image is transmitted using a UFMC-assisted NOMA scheme. The proposed approach is evaluated for several medical images and compared with competing schemes by various tests that were performed. It was found that PSNR is above 69 dB, and NCC is above 0.99. It has been demonstrated that the proposed watermarking technique produces better watermark imperceptibility and robustness under various attacks. Also, the minimum execution time achieved for the embedding and extracting processes is about 0.3284 Sec.. In addition, the performance analysis of the proposed method in terms of BER shows good behaviour under a wireless fading channel. Finally, the polar code is employed for many purposes, including watermarking, security, and ECC, making

the proposed scheme a promising solution for protecting the privacy of medical images.

## Conflicts of Interest

The authors declare that there is no conflict of interest.

## Author Contributions

Conceptualization, methodology, software, validation, formal analysis, investigation, resources, data curation, writing-original preparation, writing review, editing, and visualization have been implemented by the 1st ,2nd and 3rd authors.

## References

[1] D. Li, Y. w. Chen, J. Li, L. Cao, U. A. Bhatti, and P. Zhang, "Robust watermarking algorithm for medical images based on accelerated-KAZE discrete cosine transform", *IET Biometrics*, Vol. 11, No. 6, pp. 534-546, 2022.
[2] S. Sharma, J. J. Zou, and G. Fang, "A dual watermarking scheme for identity protection", *Multimedia Tools and Applications*, Vol. 82, No. 2, pp. 2207-2236, 2023.
[3] S. Gull and S. A. Parah, "Advances in medical image watermarking: a state of the art review", *Multimedia Tools and Applications*, Vol. 83, No. 1, pp. 1406-1447, 2023.

[4] X. Zhou, H. Zhang, and C. Wang, "A robust image watermarking technique based on DWT, APDCBT and SVD", *Symmetry*, Vol. 10, No. 3, p. 77, 2018.

[5] M. H. Kabir, J. Rahman, and S. E. Ullah, "Secured voice frequency signal transmission in 5G compatible multiuser downlink MIMO NOMA wireless communication system", *International Journal of Networks and Communications*, Vol. 8, No. 4, pp. 97-105, 2018.

[6] M. Gupta, A. S. Kang, and V. Sharma, "Comparative Study on Implementation Performance Analysis of Simulink Models of Cognitive Radio Based GFDM and UFMC Techniques for 5G Wireless Communication", *Wireless Personal Communications*, pp. 135-165, Vol. 126, No. 1, 2020.

[7] D. Pokamestov, Y. Kryukov, E. Rogozhnikov, G. Shalin, A. Shinkevich, and S. Novichkov, "Adaptation of Signal with NOMA and Polar Codes to the Rayleigh Channel", *Symmetry*, Vol. 14, No. 10, p. 2103, 2022.

[8] M. J. M. Ameen and S. S. Hreshee, "Security analysis of encrypted audio based on elliptic curve and hybrid chaotic maps within GFDM modulator in 5G networks", *Bulletin of Electrical Engineering and Informatics*, Vol. 12, No. 6, pp. 3467-3479, 2023.

[9] A. K. Singh, B. Kumar, M. Dave, and A. Mohan, "Robust and imperceptible dual watermarking for telemedicine applications", *Wireless Personal Communications*, Vol. 80, pp. 1415-1433, 2015.

[10] A. K. Singh, B. Kumar, M. Dave, and A. Mohan, "Multiple watermarking on medical images using selective discrete wavelet transform coefficients", *Journal of Medical Imaging and Health Informatics*, Vol. 5, No. 3, pp. 607-614, 2015.

[11] R. Thanki, S. Borra, V. Dwivedi, and K. Borisagar, "An efficient medical image watermarking scheme based on FDCuT-DCT", *International Journal of Engineering Science and Technology*, Vol. 20, No. 4, pp. 1366-1379, 2017.

[12] A. Zear, A. K. Singh, and P. Kumar, "A proposed secure multiple watermarking technique based on DWT, DCT and SVD for application in medicine", *Multimedia tools and applications*, Vol. 77, pp. 4863-4882, 2018.

[13] S. Prajwalasimha, S. Chethan Suputhra, and C. Mohan, "Performance analysis of DCT and successive division based digital image watermarking scheme", *Indonesian Journal of Electrical Engineering and Computer Science*, Vol. 15, No. 2, pp. 750-757, 2019.

[14] H.-J. Ko, C.-T. Huang, G. Horng, and W. Shiuh-Jeng, "Robust and blind image watermarking in DCT domain using inter-block coefficient correlation", *Information Sciences*, Vol. 517, pp. 128-147, 2020.

[15] N. Zermi, A. Khaldi, M. R. Kafi, F. Kahlessenane, and S. Euschi, "A lossless DWT-SVD domain watermarking for medical information security", *Multimedia Tools and Applications*, Vol. 80, pp. 24823-24841, 2021.

[16] M. Tang and F. Zhou, "A robust and secure watermarking algorithm based on DWT and SVD in the fractional order fourier transform domain", *Array*, Vol. 15, p. 100230, 2022.

[17] W. Alomoush et al., "Digital image watermarking using discrete cosine transformation based linear modulation", *Journal of Cloud Computing*, Vol. 12, No. 1, pp. 1-17, 2023.

[18] X. Zhang, Z. Wang, X. Ning, and H. Xie, "On the performance of GFDM assisted NOMA schemes", *IEEE Access*, Vol. 8, pp. 88961-88968, 2020.

[19] R. S. Yarrabothu, N. Kanchukommula, and U. R. Nelakuditi, "Design and Analysis of Universal-Filtered Multi-carrier (UFMC) Waveform for 5G Cellular Communications Using Kaiser Filter", *Soft Computing and Signal Processing: Proceedings of ICSCSP, Singapore*, Vol. 2, 2019: Springer, pp. 721-730, 2018,

[20] S. Wei, H. Li, W. Zhang, and W. Cheng, "A comprehensive performance evaluation of universal filtered multi-carrier technique", *IEEE Access*, Vol. 7, pp. 81429-81440, 2019.

[21] Z. Babar et al., "Polar codes and their quantum-domain counterparts", *IEEE Communications Surveys & Tutorials*, Vol. 22, No. 1, pp. 123-155, 2019.

[22] M. Ali, C. W. Ahn, and M. Pant, "A robust image watermarking technique using SVD and differential evolution in DCT domain", *Optik*, Vol. 125, No. 1, pp. 428-434, 2014.

[23] L. Liu and S. Miao, "An image encryption algorithm based on Baker map with varying parameter", *Multimedia Tools and Applications*, Vol. 76, pp. 16511-16527, 2017.

[24] M. J. M. Ameen and S. S. Hreshee, "Hyperchaotic Based Encrypted Audio Transmission via Massive MIMO-GFDM System using DNA Coding in the Antenna Index of PSM", In: *Proc. of 5th International Conference on Engineering Technology and its Applications (IICETA)*, Najaf, Iraq, pp. 19-24, 2022.

[25] P.-L. Delisle, B. Anctil-Robitaille, C. Desrosiers, and H. Lombaert, "Realistic image normalization for multi-Domain segmentation", *Medical Image Analysis*, Vol. 74, p. 102191, 2021.

[26] H. Zhang, C. Wang, and X. Zhou, "A robust image watermarking scheme based on SVD in the spatial domain", *Future Internet*, Vol. 9, No. 3, p. 45, 2017.